Fermilab

NOvA Recent Results of Three-Flavor Oscillation Analysis

FERMILAB-CONF-24-0911-V

DOI:10.1134/S1063778825600654

ISSN 1063-7788, Physics of Atomic Nuclei, 2025, Vol. 88, No. 3, pp. 443–447.

ELEMENTARY PARTICLES AND FIELDS
Experiment

NOvA Recent Results of Three-Flavor Oscillation Analysis

Anastasiia Kalitkina[1)*]
(for the NOvA Collaboration)

Received December 2, 2024; revised December 2, 2024; accepted January 20, 2025

Abstract—The NOvA experiment is a long-baseline neutrino experiment designed to study the oscillation behavior of neutrinos and antineutrinos, utilizing Fermilab's Megawatt-capable NuMI neutrino beam. Over the past 10 years, NOvA has collected data from two functionally identical tracking calorimeter detectors, which are situated off the NuMI beam axis and separated by 810 km. The construction of the experiment enables observation of muon (anti)neutrino disappearance and electron (anti)neutrino appearance. Consequently, precision measurements of oscillation parameters, including the mass splitting Δm^2_{32} and its sign, the mixing angle θ_{23}, and the phase of CP-symmetry violation, can be obtained. This paper presents an overview of the NOvA experiment and its latest results.

DOI: 10.1134/S1063778825600654

1. INTRODUCTION

There are three flavor types of light neutrinos: electron, muon, and tau neutrinos. One of the key phenomena studied in neutrino physics is their oscillation, which occurs due to nonzero neutrino masses. The probability of neutrino oscillation in the three-flavor model depends on at least four parameters from the PMNS mixing matrix: three mixing angles θ_{12}, θ_{13}, θ_{23}, and a phase of charge-parity symmetry δ_{CP}; and two mass splittings Δm^2_{21} and Δm^2_{32}. Measurement of these parameters is important for understanding the fundamental properties of neutrinos and has implications for our understanding of the universe, including the matter-antimatter asymmetry.

Each neutrino experiment uniquely contributes to our understanding of oscillation parameters. The NOvA experiment [1] is designed for precise measurements over long distances. It utilizes the NuMI accelerator facility at Fermilab as its neutrino source, which can provide either a neutrino or an antineutrino beam. In this facility, 120 GeV accelerated protons are directed at a target, where secondary mesons decay and produce a beam consisting almost entirely of muon neutrinos or antineutrinos, depending on the horn current in the focusing system. NOvA consists of two tracking calorimeter detectors, which have similar construction but differ in size and purpose. Both detectors are constructed from PVC cells, filled with liquid scintillator. The Near Detector (ND) is located approximately 1 km from the source to measure the unoscillated neutrino beam composition, while the oscillated neutrino flux is measured by the Far Detector (FD) at a distance of 810 kilometers. Both ND and FD are placed 14.6 mrad off the beamline, which reduces the number of high-energy neutrinos and forms a narrow energy peak at about 2 GeV.

NOvA started collecting data in 2014, with an average beam power of about 700 kW. Since the NuMI beam is being upgraded for future long-baseline neutrino oscillation experiments at Fermilab, the current average beam power has risen to nearly 1 MW. There is a linear dependence between the beam power and the number of protons delivered on the target (POT), which characterizes the exposure of accelerator neutrino experiments. The latest three-flavor neutrino analysis includes the 10 years of NOvA data, corresponding 26.61×10^{20} POT of neutrino data and 12.50×10^{20} POT of antineutrino data. Compared to the previous major results in 2020 [2], the exposure of the neutrino beam has been doubled.

2. EVENT SELECTION

NOvA was designed to study two channels: muon (anti-)neutrino disappearance and electron (anti-)neutrino appearance. The first process, $\nu_\mu \to \nu_\mu$ ($\bar{\nu}_\mu \to \bar{\nu}_\mu$), is sensitive to the mixing angle θ_{23} and the mass splitting Δm^2_{32}. The mixing angle modulates the FD spectra and characterizes the proportions of ν_μ and ν_τ in the third neutrino mass eigenstate. The magnitude of Δm^2_{32} defines the shift of the oscillation probability minimum. Sensitivity to these parameters is also present in the second process, $\nu_\mu \to \nu_e$ ($\bar{\nu}_\mu \to \bar{\nu}_e$). However, the appearance channel has additional mild sensitivity to the

[1)]Joint Institute for Nuclear Research, Dubna, Russia.
[*]E-mail: kalitkina@jinr.ru

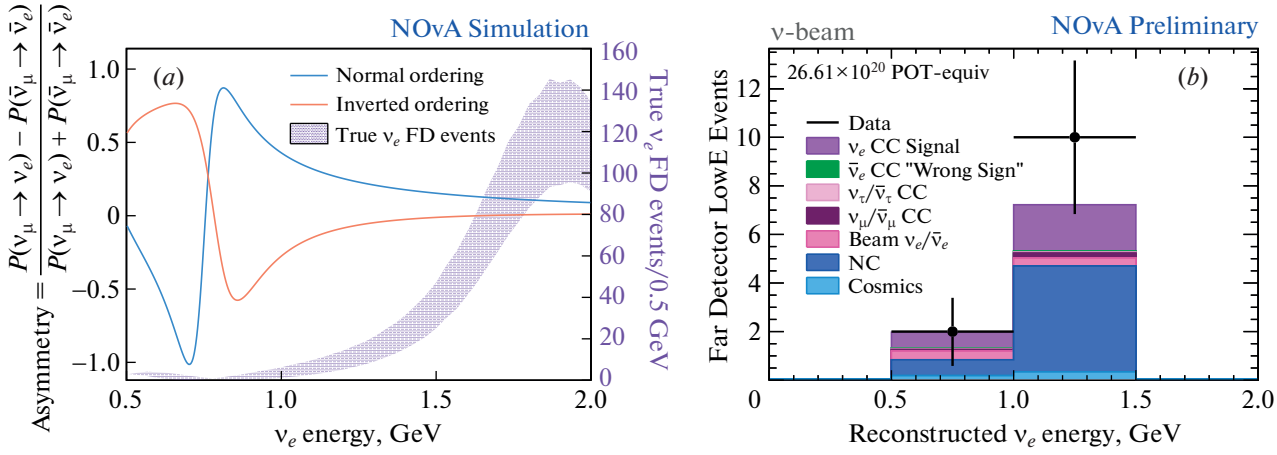

Fig. 1. Low energy electron neutrino sample: (*a*) Oscillation probability asymmetry under the assumption of normal and inverted mass ordering; (*b*) Electron neutrino spectrum in the FD showing background composition and data points.

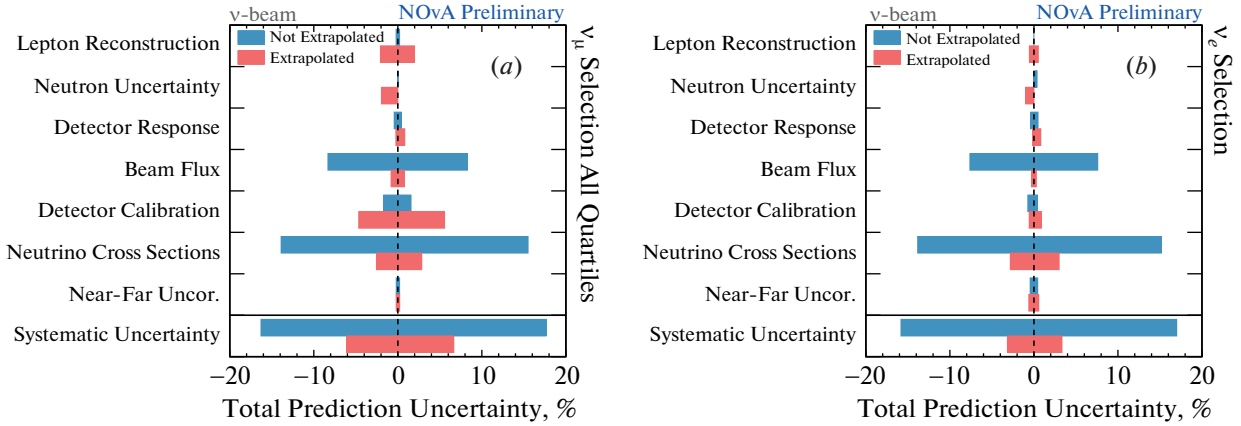

Fig. 2. Summary of all systematic uncertainties for both (*a*) ν_μ and (*b*) ν_e predictions in the FD. The two bars compare predictions with (red) and without (blue) the extrapolation technique.

mixing angle θ_{13}, the sign of Δm^2_{32} (neutrino mass ordering), and the CP-violating phase δ_{CP} . There is an asymmetry between ν_e and $\bar{\nu}_e$ underground propagation to the FD due to the matter effect. This asymmetry can significantly enhance the sensitivity of the analysis to neutrino mass ordering. As shown in Fig. 1*a*, in the energy region from 0.5 to 1.5 GeV, the asymmetry curve under the assumption of normal mass ordering differs drastically from that of the inverted ordering.

For the analysis, two neutrino event topologies—muon-like and electron-like—are selected as signals in both detectors and beam configurations. The full FD selection chain includes quality and containment cuts, cosmic rejection, and an event classifier [3] based on machine learning algorithms. There are strategies increasing analysis sensitivity for each event topologies. For $\nu_\mu(\bar{\nu}_\mu)$ events, sensitivity primarily depends on the shape of the energy spectrum. Thus, the selected sample is divided into four quartiles by hadronic energy fraction, where each quartile has its own energy resolution. For $\nu_e(\bar{\nu}_e)$ events, sensitivity depends on ability to separate signal from background. This sample has a relatively small number of events, so each additional neutrino can have an impact. Based on this fact, the appearance channel includes not only core samples of events with low and high particle identification (PID) scores but also an additional analysis bin for peripheral events [4], as well as, for the latest analysis, a brand new low-energy neutrino sample. This sample, shown in Fig. 1*b*, incorporates events with energies ranging from 0.5 to 1.5 GeV, which were previously excluded from the analysis.

3. FAR DETECTOR PREDICTION AND DATA

Since the detectors are functionally identical, an extrapolation technique is used. This approach produces FD predictions by propagating the differences

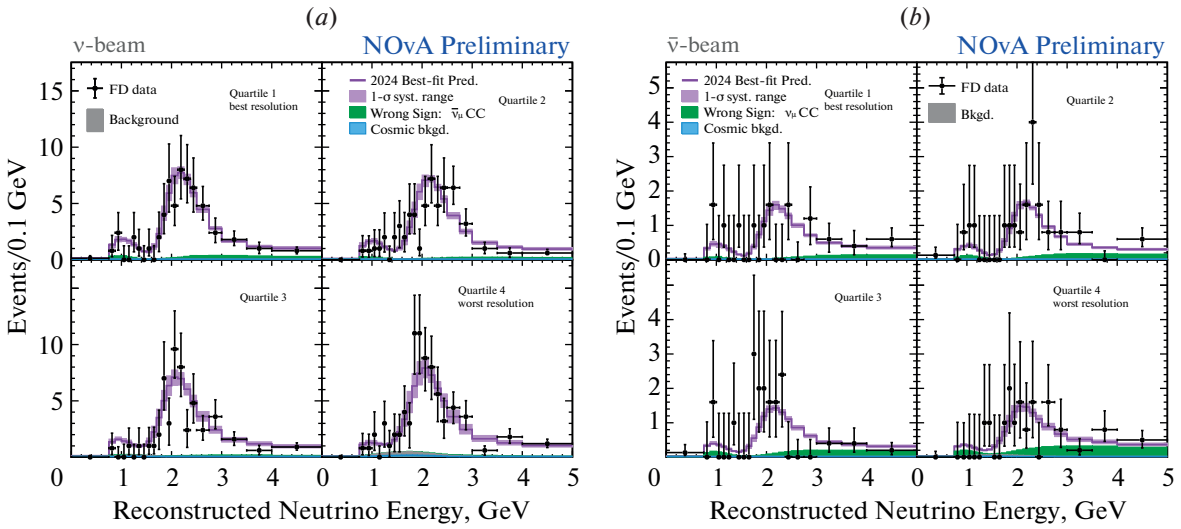

Fig. 3. FD energy spectra for (*a*) ν_μ and (*b*) $\bar{\nu}_\mu$, divided into four quartiles. Black dots represent observed data, while the violet line with 1-σ systematic uncertainties band shows Monte Carlo predictions.

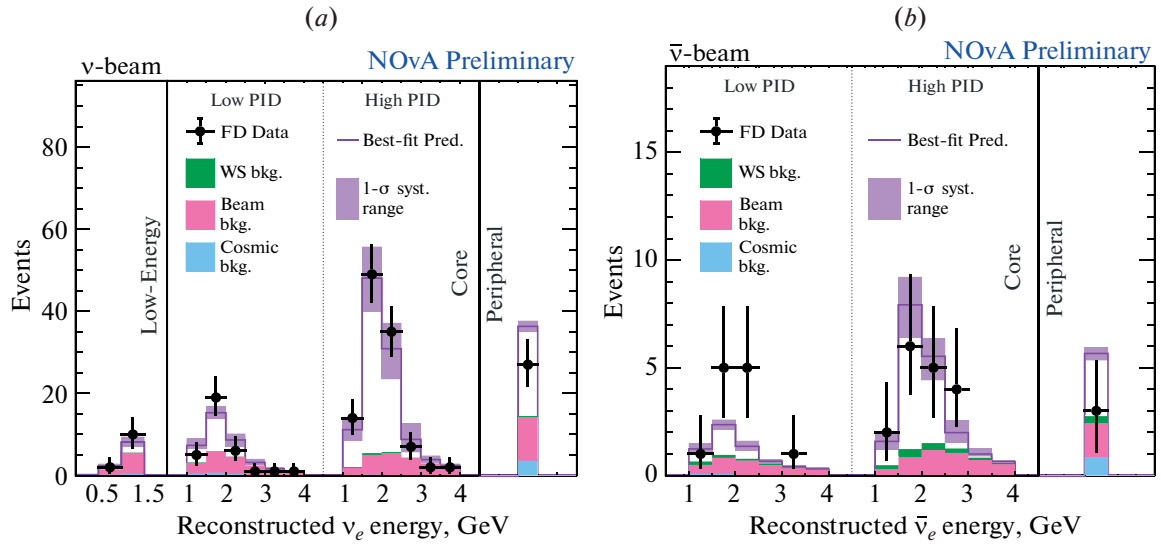

Fig. 4. FD energy spectra for (*a*) ν_e and (*b*) $\bar{\nu}_e$, divided into analysis bins. Black dots represent observed data, while the violet line with 1-σ systematic uncertainties band shows Monte Carlo predictions.

between ND data and simulation. A Far-to-Near transformation accounts for differences between detectors, and then oscillation effects are applied. As a result, total prediction systematic uncertainties are reduced from ∼18% to ∼4% for both $\nu_\mu(\bar{\nu}_\mu)$ and $\nu_e(\bar{\nu}_e)$ selections (Fig. 2).

The observed FD data of $\nu_\mu(\bar{\nu}_\mu)$ disappearance and $\nu_e(\bar{\nu}_e)$ appearance are displayed in Figs. 3 and 4, respectively. These figures also show Monte Carlo predictions with 1-σ systematic uncertainty bands. Over a 10-year period, the experiment detected 384 ν_μ and 106 $\bar{\nu}_\mu$ candidates, with expected total backgrounds of 11 and 1.7 events, respectively. In the appearance channel, 181 ν_e and 32 $\bar{\nu}_e$ candidates were observed, with corresponding expected backgrounds of 62.5 and 12.2 events.

4. ANALYSIS RESULTS

The main idea of the analysis is to compare extrapolated predictions with selected muon-like and electron-like (anti-)neutrino FD data. To achieve this, a binned likelihood function is determined as a function of the oscillation parameters, such as $\sin^2\theta_{23}$, $\sin^2\theta_{13}$, Δm^2_{32}, and δ_{CP}, along with systematic nuisance parameters. The latest analysis fit has been performed simultaneously on all 15 samples: 4 quartiles of both ν_μ and $\bar{\nu}_\mu$, low and high PID core

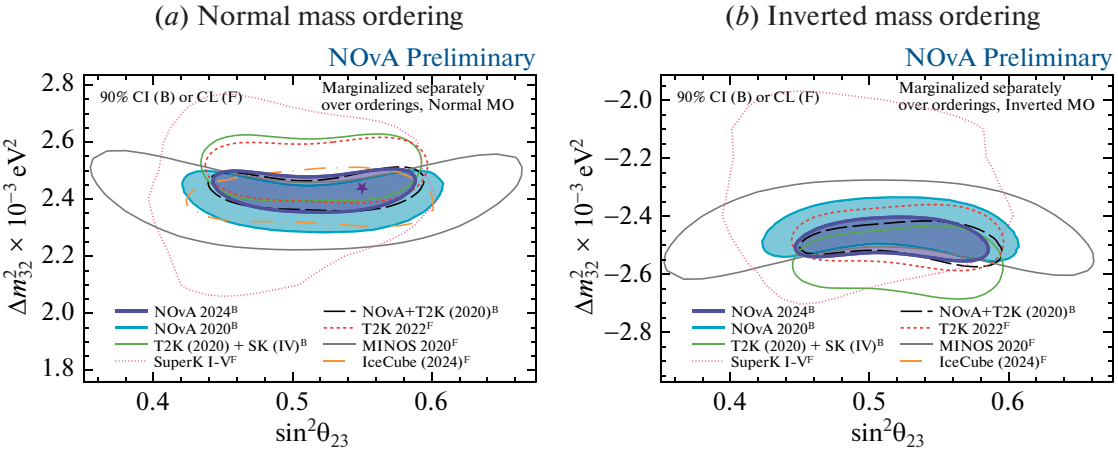

Fig. 5. Comparison of the 90% Bayesian credible intervals and confidence levels for $\sin^2\theta_{23}$ and Δm^2_{32} across various accelerator and atmospheric experiments, as well as joint analyses.

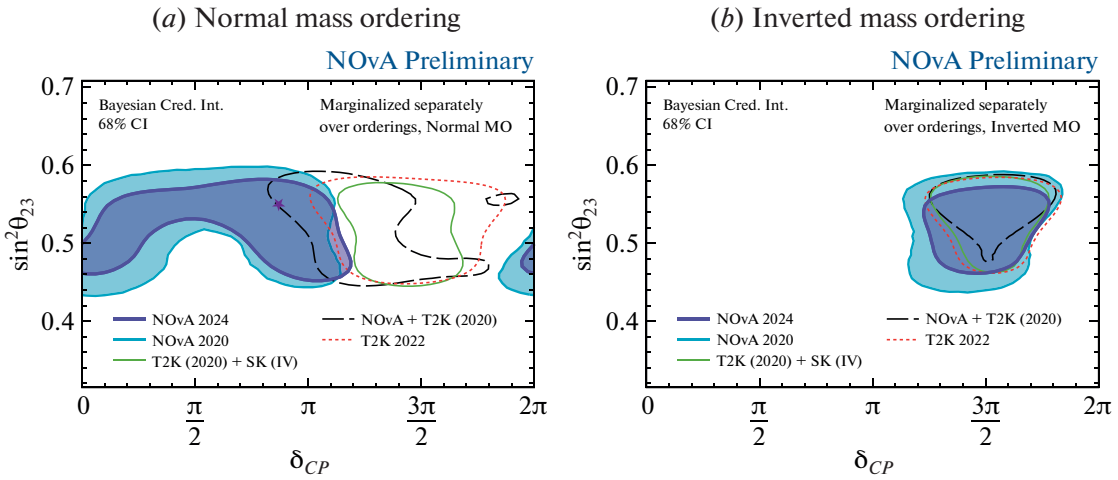

Fig. 6. Comparison of the Bayesian 1-σ credible intervals for δ_{CP} and $\sin^2\theta_{32}$.

and peripheral samples of both ν_e and $\bar{\nu}_e$, and ν_e low energy sample.

Historically, NOvA has utilized a frequentist approach using the Feldman-Cousins method [5] to derive constraints on oscillation parameters by profiling systematic nuisance parameters. Since 2022, a complementary Bayesian statistical technique has also been integrated into the NOvA analysis [6]. Furthermore, NOvA uses external constraints on the solar parameters, such as θ_{12} and Δm^2_{21}, as well as the reactor parameter θ_{13}. However, the latest analysis has been performed with three options for reactor constraints: using only NOvA data, incorporating a one-dimensional (1D) constraint on θ_{13} from Daya Bay, and applying a two-dimensional (2D) constraint on the pair of θ_{13} and Δm^2_{32} from Daya Day [7].

The best fit values of oscillation parameters from the frequentist fit of the 10-years of NOvA data with a 1D constraint on θ_{13} are $\Delta m^2_{32} = 2.433^{+0.035}_{-0.036} \times 10^{-3}$ eV^2, $\sin^2\theta_{23} = 0.546^{+0.032}_{-0.075}$, $\delta_{CP} = 0.88\pi$. The data mildly prefer normal mass ordering, the upper octant of θ_{23}, and CP-conserving δ_{CP} values. Both frequentist and Bayesian techniques have yielded similar results on the NOvA data and are consistent with previous 2020 analysis result [2]. The 2D credible intervals for the pairs ($\sin^2\theta_{23}$, Δm^2_{32}) and (δ_{CP}, $\sin^2\theta_{23}$) from the Bayesian analysis are displayed in Fig. 5 and Fig. 6, respectively. These figures also show constraints on parameter pairs from other accelerator and atmospheric experiments, as well as from joint analyses. Noticing, the mass splitting Δm^2_{32} is now the most accurately known parameter of neutrino mixing. NOvA provides the most precise single-experiment measurement of this parameter, with an uncertainty of less than 1.5%. As shown in Fig. 6, the NOvA data still disfavor asymmetry

values of δ_{CP}: in normal ordering, the area around $3\pi/2$ is excluded, but this is not the case in inverted ordering. Hence, there is tension between NOvA and T2K assuming normal mass ordering.

FUNDING

The reported study has been performed by the NOvA collaboration, using the resources from the Fermi National Accelerator Laboratory (Fermilab), a U.S. Department of Energy, Office of Science, HEP User Facility, as well as the Dzhelepov Laboratory of Nuclear Problems at the Joint Institute for Nuclear Research.

CONFLICT OF INTEREST

The author of this work declares that she has no conflicts of interest.

OPEN ACCESS

REFERENCES

1. D. S. Ayres, G. R. Drake, M. C. Goodman, J. J. Grudzinski, V. J. Guarino, R. L. Talaga, A. Zhao, P. Stamoulis, E. Stiliaris, G. Tzanakos, et al. (NOvA Collaboration), The NOvA Technical Design Report (Office of Scientific and Technical Information (OSTI), 2007).
https://doi.org/10.2172/935497
2. M. A. Acero, P. Adamson, L. Aliaga, N. Anfimov, A. Antoshkin, E. Arrieta-Diaz, L. Asquith, A. Aurisano, A. Back, C. Backhouse, M. Baird, N. Balashov, P. Baldi, et al. (NOvA Collaboration), Phys. Rev. D **106**, 32004 (2022).
https://doi.org/10.1103/physrevd.106.032004
3. A. Aurisano, A. Radovic, D. Rocco, A. Himmel, M. D. Messier, E. Niner, G. Pawloski, F. Psihas, A. Sousa, and P. Vahle, J. Instrum. **11**, P09001 (2016).
https://doi.org/10.1088/1748-0221/11/09/p09001
4. M. A. Acero, P. Adamson, L. Aliaga, T. Alion, V. Allakhverdian, N. Anfimov, A. Antoshkin, E. Arrieta-Diaz, A. Aurisano, A. Back, C. Backhouse, M. Baird, et al. (NOvA Collaboration), Phys. Rev. D **98**, 32012 (2018).
https://doi.org/10.1103/physrevd.98.032012
5. M. A. Acero, B. Acharya, P. Adamson, L. Aliaga, N. Anfimov, A. Antoshkin, E. Arrieta-Diaz, L. Asquith, A. Aurisano, A. Back, C. Backhouse, M. Baird, N. Balashov, P. Baldi, B. A. Bambah, S. Bashar, A. Bat, K. Bays, et al. (NOvA Collaboration), J. Instrum. **20**, T02001 (2025).
https://doi.org/10.1088/1748-0221/20/02/t02001
6. M. A. Acero, B. Acharya, P. Adamson, N. Anfimov, A. Antoshkin, E. Arrieta-Diaz, L. Asquith, A. Aurisano, A. Back, N. Balashov, P. Baldi, B. A. Bambah, A. Bat, K. Bays, R. Bernstein, T. J. C. Bezerra, V. Bhatnagar, D. Bhattarai, B. Bhuyan, et al. (NOvA Collaboration), Phys. Rev. D **110**, 12005 (2024).
https://doi.org/10.1103/physrevd.110.012005
7. F. P. An, W. D. Bai, A. B. Balantekin, M. Bishai, S. Blyth, G. F. Cao, J. Cao, J. F. Chang, Y. Chang, H. S. Chen, H. Y. Chen, S. M. Chen, Y. Chen, Y. X. Chen, et al. (Daya Bay Collaboration), Phys. Rev. Lett. **130**, 161802 (2023).
https://doi.org/10.1103/physrevlett.130.161802

AI tools may have been used in the translation or editing of this article.